Agriculture, Ecosystems and Environment 240 (2017) 171–181

Contents lists available at ScienceDirect

Agriculture, Ecosystems and Environment

journal homepage: www.elsevier.com/locate/agee

Relationship between paired ecosystem services in the grassland and agro-pastoral transitional zone of China using the constraint line method

Ruifang Hao[a,b], Deyong Yu[a,b,*,1], Jianguo Wu[a,c]

[a] Center for Human-Environment System Sustainability (CHESS), State Key Laboratory of Earth Surface Processes and Resource Ecology (ESPRE), Beijing Normal University, Beijing 100875, China
[b] College of Resources Science & Technology, Faculty of Geographical Science, Beijing Normal University, Beijing 100875, China
[c] School of Life Sciences and School of Sustainability, Arizona State University, Tempe, AZ 85287-4501, USA

ARTICLE INFO

Article history:
Received 11 September 2016
Received in revised form 17 January 2017
Accepted 13 February 2017
Available online 24 February 2017

Keywords:
Tradeoff
Synergy
Scatter cloud
Ecological process
Scale effect
Threshold

ABSTRACT

Understanding the relationships between ecosystem services is important for promoting ecosystem service management and sustainable development. The relationships between ecosystem services have commonly been characterized as tradeoffs and synergies. Here, we report that a third type of relationship also exists, in which one ecosystem service constrains the other. Selecting the grassland and agro-pastoral transitional zone of North China (GAPTZ) as the study area, we examined the relationships between paired ecosystem services: net primary productivity (NPP), soil conservation (SC), soil erosion by wind (SL), water yield (WY), and water retention (WR). The constraint effect of one ecosystem service on the other was determined by extracting the upper constraint lines from the scatter plots of the paired ecosystem services with segmented quantile regression on the levels of landscape, class, and ecoregion. Our results revealed eight types of constraint effects between the ten paired ecosystem services: (1) positive linear, (2) negative linear, (3) logarithmic, (4) negative convex, (5) backward S-shaped, (6) hump-shaped, (7) convex-waved, and (8) concave-waved. At the landscape, class, and ecoregion levels, there was a hump-shaped constraint effect between NPP and SC. Precipitation was the main factor shaping the constraint line of the paired NPP-SC. The gradually increasing constraint effect of higher NPP on WY indicated that, in arid and semiarid areas, improving NPP decreases water yield. In farmland areas, the backward S-shaped constraint line of the paired NPP-SL indicates that crops, unlike forests and grasslands, could not protect soil from wind erosion. The constraint effects of SL on WY and WR are negative convex on the landscape level and convex-waved or concave-waved on the class and ecoregion levels. The constraint line approach enriches the understanding of linkages between ecosystem services and the potential drivers. The constraint effects of ecosystem services have important implications for sustainable land use planning to optimize landscapes services.

1. Introduction

The Millennium Ecosystem Assessment has stimulated many studies of ecosystem services (MA, 2005a,b). Ecosystem services are defined as the benefits that people derive from nature (Daily, 1997; Costanza et al., 1998). A natural ecosystem provides people with numerous goods and services that support human existence and wellbeing (MA, 2005a,b; Wu, 2013). However, until 2010, approximately 60% of ecosystem services were in decline (Costanza et al., 2014); a narrow focus on a subset of ecosystem services is known to result in a substantial decline in the provision of other ecosystem services (Lester et al., 2013). With changing demand in key ecosystem services, the demand for regulating and cultural ecosystem services is increasing (Buergi et al., 2015), and policy awareness in ecosystem service science has rapidly improved (Wong et al., 2015). Understanding the linkages between multiple ecosystem services is critical to regional ecological planning and management (Goldstein et al., 2012). The scale of

* Corresponding author at: State Key Laboratory of Earth Surface Processes and Resource Ecology, Center for Human-Environment System Sustainability (CHESS), Beijing Normal University, No. 19, Xinjiekouwai Street, Haidian District, Beijing, 100875, China.
E-mail addresses: hrf@mail.bnu.edu.cn (R. Hao), dyyucas@163.com (D. Yu), Jingle.Wu@asu.edu (J. Wu).
[1] Co-first author.

http://dx.doi.org/10.1016/j.agee.2017.02.015
0167-8809/

ecosystem management should match that of the ecological process that maintains the ecosystem services, otherwise ecosystem management may have an adverse effect on ecosystem services (Wu, 2004; Butler et al., 2013; Fu et al., 2013; Castro et al., 2014).

Ecologists are searching for ways to understand the relationships between ecosystem services. The relationships of ecosystem services are often characterized as tradeoffs or synergies (Bennett et al., 2009). Tradeoffs between ecosystem services occur when the provision of one ecosystem service increases at the expense of another service (Bennett et al., 2009; Raudsepp-Hearne et al., 2010). Synergies occur when multiple ecosystem services increase or decrease simultaneously (Bennett et al., 2009). Several methods have been used to characterize these relationships. An overlay analysis of ecosystem services reveals their spatial distributions, such that the hotpots and areas of tradeoff can be identified (Bai et al., 2011; Qiu and Turner, 2013). Several studies have used the Pareto Efficiency and the Efficiency Frontier methods to analyze these tradeoffs, but these studies were mostly performed as hypothetical or theoretical analyses (Sanon et al., 2012; Lester et al., 2013; Ruijs et al., 2013). Some statistical methods, such as regression analysis and bagplot, have been used to analyze tradeoffs and synergies between ecosystem services (Jia et al., 2014; Jopke et al., 2015; Wu et al., 2015; Favretto et al., 2016). Among a variety of statistical methods, most studies used a correlation coefficient to determine whether ecosystem services were related (Raudsepp-Hearne et al., 2010; Jopke et al., 2015). A correlation analysis is simple and directly reflects the strength of the relationships. However, a correlation analysis assumes that the relationships between ecosystem services are monotonous, which is not true in many cases. The correlation coefficients reflect only general trends in paired ecosystem services. When there are many sample points, the scatter points tend to distribute similar to a cloud and vary over a large range in the scatter plots of the paired ecosystem services (Raudsepp-Hearne et al., 2010; Jia et al., 2014). Such scatters cannot be interpreted by traditional correlation or regression because the large variance of the scatters is converse to the assumption of variance homogeneity of correlation (Cade and Guo, 2000).

Whether the current statistical methods are appropriate to represent the relationships between ecosystem services is seldom discussed. For each ecosystem service, there are many impact factors, including climate factors, land use/cover change, and other ecosystem services (Bennett et al., 2009). Because of the complex interaction among multiple factors, it is difficult to measure the linkage of ecosystem services with linear thinking.

The GAPTZ acts as an ecological protective belt for Eastern China's agricultural plain and metropolitan areas (Gao et al., 2000). In the GAPTZ, the ecosystem services are diverse and abundant, i.e., the carbon sequestration capacity, livestock products, and recreation and entertainment (Qiu and Tang, 2003). With climate change and increasing human activity, the vulnerable ecosystem of the GAPTZ is under great pressure. Because of improvements in policy awareness protecting ecosystems in the GAPTZ, the provision of ecosystem services has changed greatly (Fu et al., 2005; Jiang et al., 2016). To achieve reasonably ecological management, it is important to understand the linkage between key ecosystem services on different scales in the GATPZ. The GAPTZ is a rational site to study the relationship between ecosystem services under complicate drivers. Many studies have estimated ecosystem services in the GAPTZ, such as soil conservation, soil loss by wind, and soil organic carbon stock (Gong et al., 2014; Wu et al., 2015), and analyzed the tradeoffs and synergies between ecosystem services using correlation analyses (Zheng et al., 2014), regression analyses (Jia et al., 2014; Li et al., 2016), and the root mean square error method (Lu et al., 2014; Zhang et al., 2015). However, the complex interaction between ecosystem services and its scale effect have not been reported. In this study, we introduced a new perspective concerning the constraint effects to enrich the understanding of the relationship between ecosystem services. The main objectives of this study are to 1) define the types of constraint effects between ecosystem services, 2) initiate a quantitative method to identify the types of constraint effects between ecosystem services across different scales in the GAPTZ,

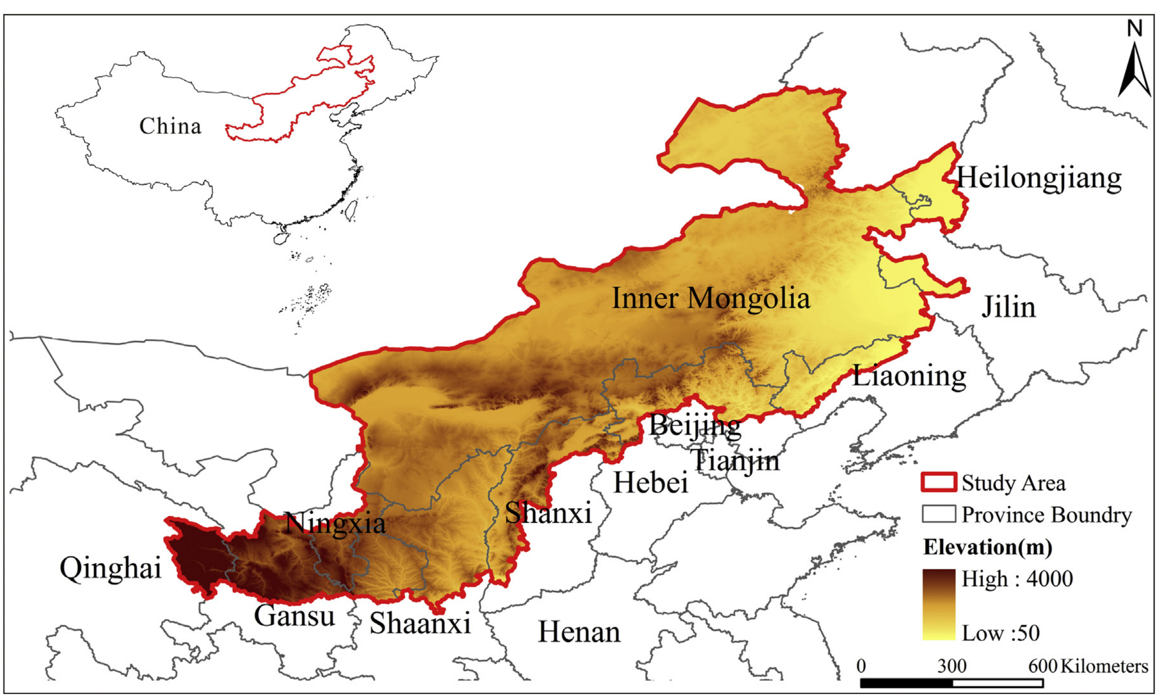

Fig. 1. The location of the grassland and agro-pastoral transitional zone of North China (GAPTZ).

and 3) discuss the implications of the constraint line approach in optimizing regional ecosystem services.

2. Materials and methods

2.1. Study area

The GAPTZ is located in the arid and semiarid region comprising 120 million km^2, with annual mean precipitation of 200 mm–400 mm (Wang et al., 1999; Zhang and Shi, 2003). The region spans 11 provinces (Fig. 1). The landscape of the region consisted of 55% grassland, 10% forest, 24% farmland, and 11% other land use/cover types in 2000 (Fig. 2(a)). The slope in the region ranges from 0 to 26°, and the main terrain is upland plain (Fig. 2(b)). The GAPTZ contains four ecoregions, including broadleaf deciduous forest (BDF), meadow steppe (MS), typical steppe (TS), and desert and desert steppe (DDS) (Fig. 2(c)). Loam and sand are the main soil types (Fig. 2(d)).

2.2. Definition of the types of constraint effects between ecosystem services

In ecology, bivariate scatter plots convey ecological information when the scatter clouds contain informative edges, which are referred to as constraint lines (Blackburn et al., 1992; Thomson et al., 1996; Horning, 2012). A constraint line represents the distribution range or potential maximum of the response variable with the effect of the constraint factor (Webb, 1972; Mills et al., 2006). Compared with most conventional methods, constraint lines are better able to characterize the effects of major constraint processes in complex systems, in which many factors contribute to the response variables (Jansen et al., 2007; Roberts and Angermeier, 2007). Points on the constraint lines indicate that the response variable is constrained by a constraint factor, with less or almost no constraint by any other factors (Evanylo and Sumner, 1987; Guo et al., 1998; Mills et al., 2009). The constraint effect of paired ecosystem services means that one ecosystem service (constraint variable) constrains the other (response variable). In the scatter clouds of paired ecosystem services, we can extract boundary points to fit constraint lines. The constraint line represents the potential scope of the response ecosystem service under the effect of the constraint ecosystem service. Points below the constraint line indicate that the relationship between paired ecosystem services is much more impacted by other factors.

The common types of constraint effects between paired ecosystem services are defined in Fig. 3. (a) Positive linear: the constraint effect of variable x on variable y is proportionally decreasing. (b) Negative linear: the variable x could effectively constrain the variable y with a proportionally increasing constraint effect. (c) Positive convex: as the variable x increases, its constraint effect on the variable y gradually decreases. (d) Negative convex: the constraint effect gradually increases. (e) Exponential: the constraint effect of the variable x on the variable y continues to decrease throughout the whole range. (f) Logarithmic: the constraint effect of the variable x on the variable y gradually increases. (g) S-shaped curve: as the variable x increases, its constraint effect on the variable y sharply decreases over some range of x. (h) Backward S-shaped: over some range of x, there is almost no constraint effect. Over a threshold, the constraint effect sharply increases. (i) Hump-shaped: with an increase in x, the constraint effect first decreases and then increases. (j) U-shaped: it is opposite of hump-shaped constraint line. (k) Convex-waved and (l) concave-waved: the constraint effect of x on y exhibits fluctuating features. They may consist of a number of hump-

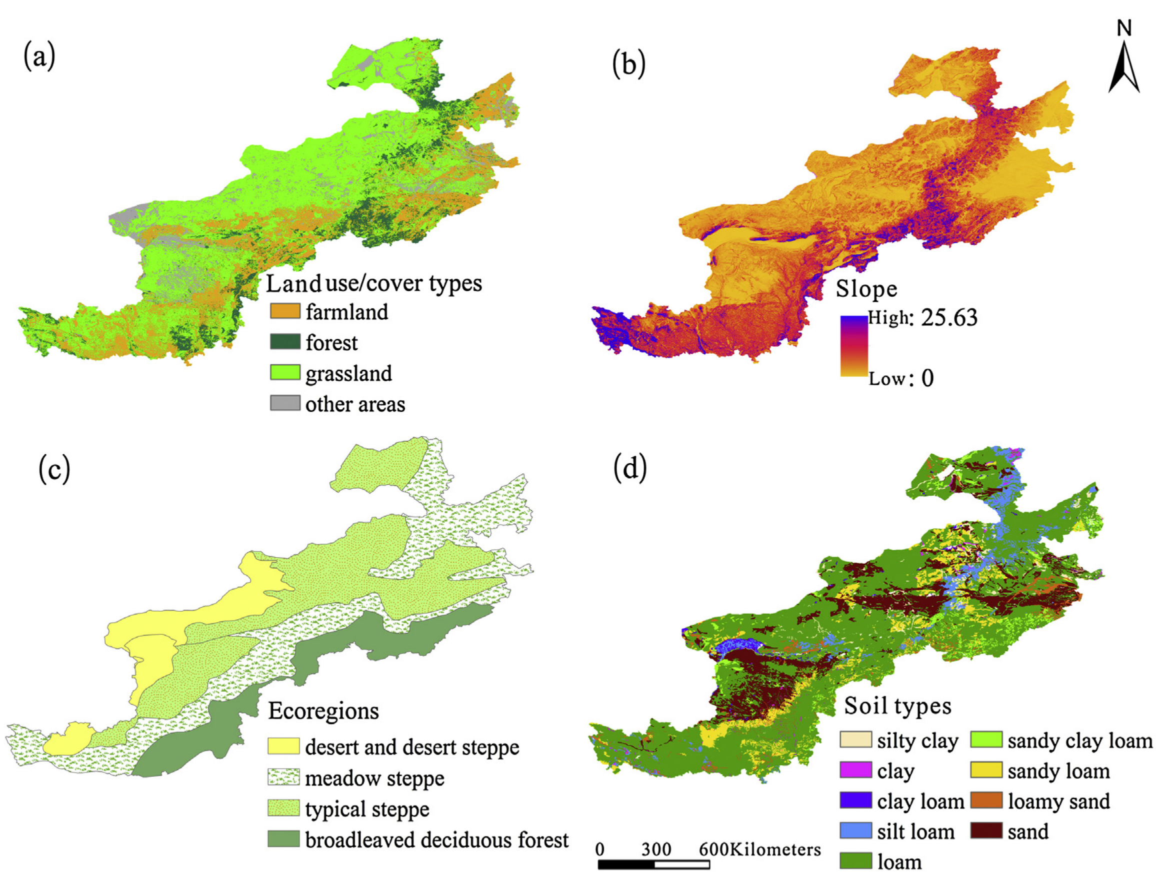

Fig. 2. Ecological context of the study area, including (a) land use/cover types in 2000, (b) the spatial distribution of slope, (c) ecoregions of the study area, and (d) soil types.

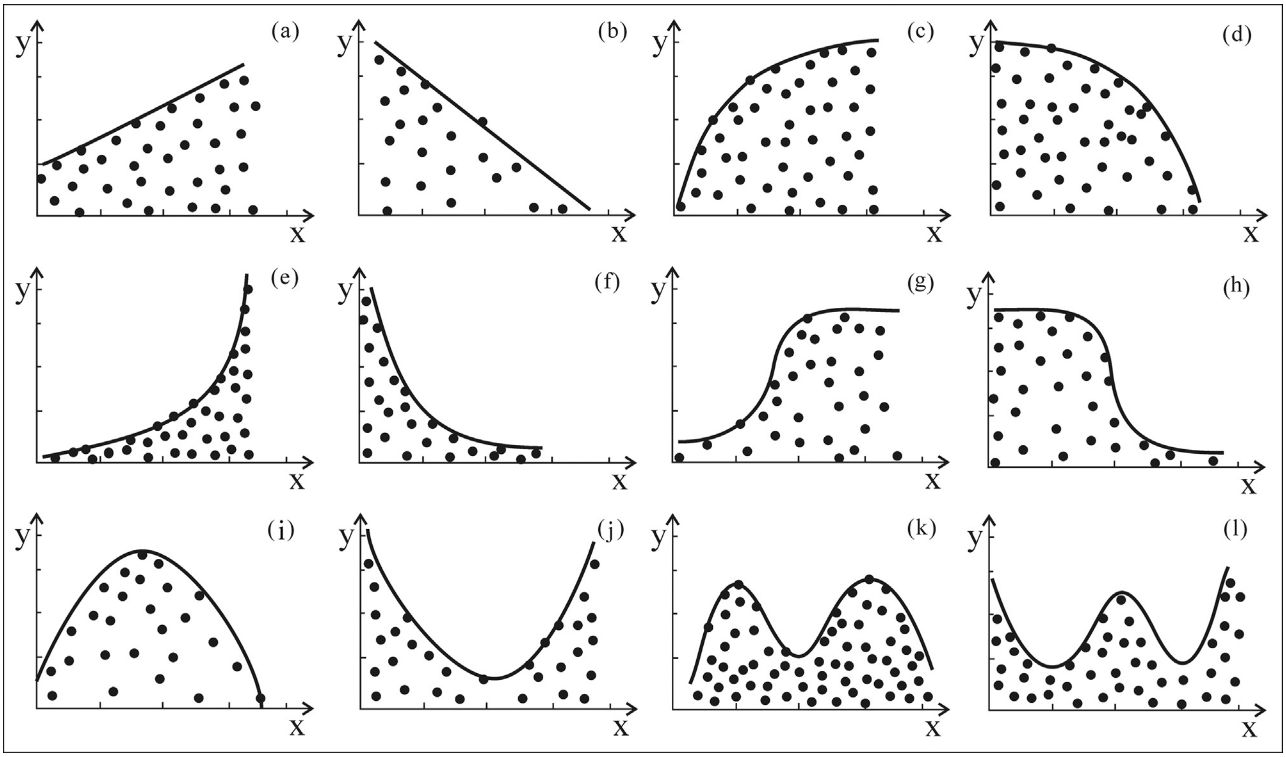

Fig. 3. The types of constraint effects between ecosystem services. (a) Positive linear line, (b) negative linear line, (c) positive convex curve, (d) negative convex curve, (e) exponential curve, (f) logarithmic curve, (g) S-shaped curve, (h) backward S-shaped curve, (i) hump-shaped curve, (j) U-shaped curve, (k) convex-waved curve, and (l) concave-waved curve.

shaped curves or U-shaped curves. The non-monotonic types of (i), (j), (k), and (l) are the result of different dominant factors on the two sides of the thresholds.

2.3. Estimation of ecosystem services

In this study, we estimated the following five annual ecosystem services with a 1 km spatial resolution: net primary productivity (NPP), soil conservation (SC), soil erosion by wind (SL), water yield (WY), and water retention (WR). Climate data, terrain data, soil data, and land use/cover data were used. Table 1 provides a brief description of the datasets. All climate datasets were spatially interpolated to a 1 km spatial resolution before they were input into the ecosystem service models.

2.3.1. Net primary productivity

NPP is an important component of the terrestrial carbon cycle. In this study, NPP was estimated using the Carnegie-Ames-Stanford Approach (Potter et al., 1993), based on Geographic Information Systems and remote sensing data. The model is expressed as follows:

$$NPP = F(SOL, NDVI) \times \varepsilon \quad (1)$$

Table 1
Description of the study data.

Data	Data description	Data source
Climate data	Daily mean temperature Daily maximum temperature Daily minimum temperature Daily rainfall Daily mean wind speed Daily sunshine duration	These datasets were provided by China Meteorological Sharing Service System.
DEM	Digital Elevation Model with 90 m spatial resolution	The dataset was provided by Geospatial Data Cloud, Computer Network Information Center, Chinese Academy of Sciences.
Ecoregion	Shape files of ecoregions in China	The dataset was provided by Data Center for Resources and Environmental Sciences, Chinese Academy of Sciences (RESDC) (http://www.resdc.cn).
Soil data	Soil texture, topsoil sand fraction, topsoil silt fraction, topsoil clay fraction, topsoil organic carbon with 1 km spatial resolution	The dataset was provided by Cold and Arid Regions Science Data Center at Lanzhou.
Land use/cover	Land use/cover with 1 km spatial resolution in 2000	The dataset was provided by Infrastructure of Earth System Science.
Normalized Difference Vegetation Index (NDVI)	Monthly NDVI with 1 km spatial resolution in 2000	The dataset was provided by Geospatial Data Cloud, Computer Network Information Center, Chinese Academy of Sciences.
Plant evapotranspiration	The plant evapotranspiration for different land use/cover types	InVEST (Integrated Valuation of Ecosystem Services and Trade-offs) User's Guide (Sharp et al., 2015)
Soil roughness	The soil roughness for different land use/cover types	Fryrear et al. (1998); Gong et al. (2014)
Crop barrier	The optical density and stand density of forest areas in 2000	Fryrear et al. (1998)

where NPP is the monthly net primary productivity ($g\,C\,m^{-2}$); SOL is the total solar radiation ($MJ\,m^{-2}$) calculated based on the daily sunshine duration; NDVI is the normalized difference vegetation index derived from moderate-resolution imaging spectroradiometer (MODIS) data; and ε is the light utility efficiency, which is determined by temperature and precipitation (Zhu et al., 2007).

2.3.2. Soil conservation

Soil erosion by water can easily be triggered by the lack of vegetation cover. It can result in soil degradation, a decline in land productivity, and the degradation of rivers, lakes, and estuaries. In this study, soil conservation was estimated using the Revised Universal Soil Loss Equation (Renard et al., 1991). This equation is expressed as follows:

$$SC = R \times K \times LS - R \times K \times LS \times C \times P \quad (2)$$

where SC is the annual soil conservation ($t\,ha^{-1}\,y^{-1}$); R is the rainfall-runoff erosivity ($MJ\,mm\,ha^{-2}\,ha^{-1}\,y^{-1}$), which is calculated based on the daily rainfall; K represents the soil erodibility factor ($t\,h\,MJ^{-1}\,mm^{-1}$); LS is the slope length and steepness factor, which is calculated based on Digital Elevation Model (DEM) using ArcGIS9.3 (Esri, US); C is a dimensionless vegetation cover factor calculated by vegetation coverage fraction (Cai et al., 2000); and P refers to the soil conservation practice using Wener's slope-based method (Wischmeier and Smith, 1965; Jia et al., 2014).

2.3.3. Water yield

Water yield is a key ecosystem service in arid and semiarid regions. Land use/cover change can have a significant impact on the hydrologic cycle by affecting the patterns of evaporation and soil infiltration. We used the integrated valuation of ecosystem services and tradeoffs (InVEST) model to assess the water yield (Sharp et al., 2015). In the InVEST model, water yield is calculated based on the water balance. It is expressed as follows:

$$WY = P - AET \quad (3)$$

where WY is the total annual water yield ($mm\,y^{-1}$); P refers to monthly precipitation ($mm\,m^{-1}$); and AET is actual evapotranspiration ($mm\,m^{-1}$) which is calculated by the following algorithm (Sharp et al., 2015).

$$AET = \frac{1 + wR_j}{1 + wR_j + \frac{1}{R_j}}P \quad (4)$$

$$R_j = \frac{k_j \times ETO}{P} \quad (5)$$

$$w = z\frac{AWC}{P} + 1.25 \quad (6)$$

$$AWC = \min(Soildepth, Rootdepth) \times PAWC \quad (7)$$

where R_j is aridity index for certain land use/cover type; k_j is the vegetation evapotranspiration coefficient associated with land use/cover type which was defined in the InVEST model (listed in Table 1); ETO is potential evapotranspiration calculated by the algorithm of FAO (Allen et al., 1998); w is non-physical parameter; AWC is the volumetric plant available water content; PAWC is the plant available water capacity calculated by the algorithm of Zhou et al. (2005); z is an hydrogeological constant computed by the method of Zhang et al. (2004).

2.3.4. Water retention

The ecosystem retains a fraction of the precipitation in the canopy, withered leaves, plant roots, and soil. In this study, water retention was also assessed using the InVEST model, which was estimated based on the water yield as follows:

$$WR = Min(1, 0.9 \times TI/3) \times Min(1, Ksat/300) \times Min(1, 249/V) \times WY \quad (8)$$

where WR is the annual water retention ($mm\,y^{-1}$); TI is a dimensionless topographic index calculated by slope and soil depth; Ksat is the soil saturated conductivity ($cm\,d^{-1}$) simulated by NeuroTheta software (The University of Sydney, Australia); and V is a velocity coefficient that varies with land use/cover types.

2.3.5. Soil erosion by wind

Soil erosion by wind is common in arid and semiarid regions and can result in a substantial decrease in the productivity of farmland and grassland. Soil erosion by wind in northern China has a substantial influence on people's lives in neighboring regions (Gao et al., 2000). The Revised Wind Erosion Equation has been extended for spatial applications in northern China based on ArcGIS (Guo et al., 2013). The model is expressed as follows:

$$Q_{max} = 109.8 \times (WF \times EF \times SCF \times K \times COG) \quad (9)$$

$$s = 150.71 \times (WF \times EF \times SCF \times K \times COG)^{-0.3711} \quad (10)$$

$$SL = 2x/s^2 Q_{max} exp\left(-(x/s)^2\right) \quad (11)$$

where Q_{max} refers to the maximum transport capacity calculated based on the climate factor (WF), soil erodibility factor (EF), soil crust factor (SCF), soil roughness (K), and combined vegetation factor (COG); s is the length of the critical field; x refers to the distance to the upwind edge of the field; and SL is the semi-monthly soil loss ($kg\,m^{-2}$) in the special case where Q_{max} and s are constant (i.e., not a function of x) (Fryrear et al., 1998).

The Carnegie-Ames-Stanford Approach, the Revised Universal Soil Loss Equation, and the Revised Wind Erosion Equation have been shown to be robust for capturing the biophysical parameters of the study area (Fu et al., 2005; Zhu et al., 2007; Guo et al., 2013). Moreover, in this study, key factors, such as the combined vegetation factor and the climate factor, were derived from remote sensing observational data and local meteorological data.

2.4. Extracting constraint lines from the scatter plots of paired ecosystem services

A segmented quantile regression was previously employed to construct constraint lines for the effects of soil properties on water infiltration (Mills et al., 2009) and on species richness (Medinski et al., 2010). In this study, the value range of ecosystem services on the *x*-axis in the scatter plot was equally divided into 100 parts to obtain 100 columns (Fig. 4). To reduce the effect of outliers, we selected the 99.9% quantile in each column as the boundary points. Thus, we obtained almost 100 boundary points to fit every constraint line. Based on the shapes of the scatter cloud and the goodness of fit values (R^2), we obtained the corresponding constraint lines using Origin 9 software (OriginLab, US). Among the constraint lines, the backward S-shaped curve, hump-shaped curve, U-shaped curve, convex-waved curve, and concave-waved curve have thresholds upon which the constraint line is segmented to indicate the direction of change of the constraint effect. The derivative equations are used to obtain the thresholds.

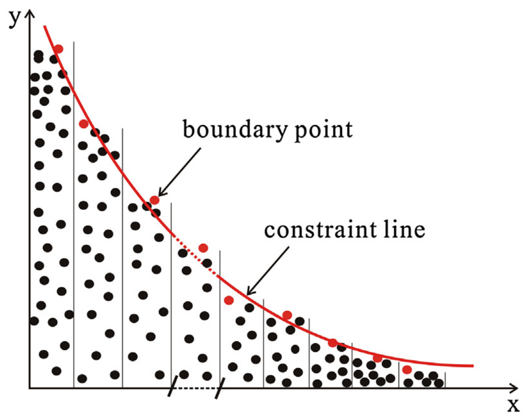

Fig. 4. Extraction of the constraint lines using the segmented quantile regression method.

NPP is one of the supporting services, and the other four services belong to regulating services (MA, 2005a). NPP is critical for sustaining livestock production and conserving regional biodiversity such this service was given special priority and was used as the constraint variable on which its effects on the other ecosystem services were studied. In addition, we also analyzed the constraint effects of SC on SL, WY, and WY; SL on WY and WR; and WY on WR.

2.5. The constraint effects between paired ecosystem services on different levels

In this study, we explored the constraint effects between paired ecosystem services on the levels of landscape, class, and ecoregion, which span a wide range of climates, soil properties, and terrain types. This allowed us to minimize the effect of local factors and enabled us to identify the trends of the constraint effects on different levels. On the class level, the three main land use/cover types included were farmland, forest, and grassland. On the ecoregion level, TS, MS, DDS, and BDF were considered. On the landscape level, we included the whole study area.

3. Results

In this study, we calculated the five ecosystem services and identified their constraint effects in both 2000 and 2010. Because the spatial patterns of ecosystem services and the shapes of constraint lines derived from paired ecosystem services for the two years were very similar, we only report the results from 2000 as a case study. The results from 2010 can be found in the supplementary materials (Fig. S.2 and Fig. S.3).

3.1. Spatial pattern of the five ecosystem services

The high values of NPP were located at the southern edge and the northeast region of GAPTZ, where the main land cover was forest (Fig. 2(a) and Fig. 5(a)). The low values of NPP were mainly found in grassland areas (Fig. 2(a) and Fig. 5(a)). The high values of SC were mainly distributed in the southwest and the central south of the GAPTZ, where the slope was relatively high (Fig. 2(b) and Fig. 5(b)). The spatial patterns of SL, WY, and WR were similar but differed from those of NPP and SC. The spatial patterns of SL, WY, and WR were consistent with that of the soil types (Fig. 2(d) and Fig. 5). The high values of SL, WY, and WR were distributed in many places where the values of SC and NPP were relatively low (Fig. 5). In the areas of higher slope, the values of SL and WR were low (Fig. 2(b) and Fig. 5).

3.2. Constraint effects between paired ecosystem services on different levels

Overall, there were eight types of constraint effects between the ten paired ecosystem services on different levels in the study area, including (1) positive linear, (2) negative linear, (3) logarithmic, (4) negative convex, (5) backward S-shaped, (6) hump-shaped, (7) convex-waved, and (8) concave-waved (Fig. 6). The segmented quantile regression captured the shapes of the constraint lines well. All constraint lines were extracted with a relatively high goodness of fit (R^2) (Fig. 6).

The constraint effects of the paired ecosystem services of WY-WR, SC-SL, SC-WY, SC-WR, NPP-WR, and NPP-SC were similar on different levels (Fig. 6). On the constraint lines, WR changed

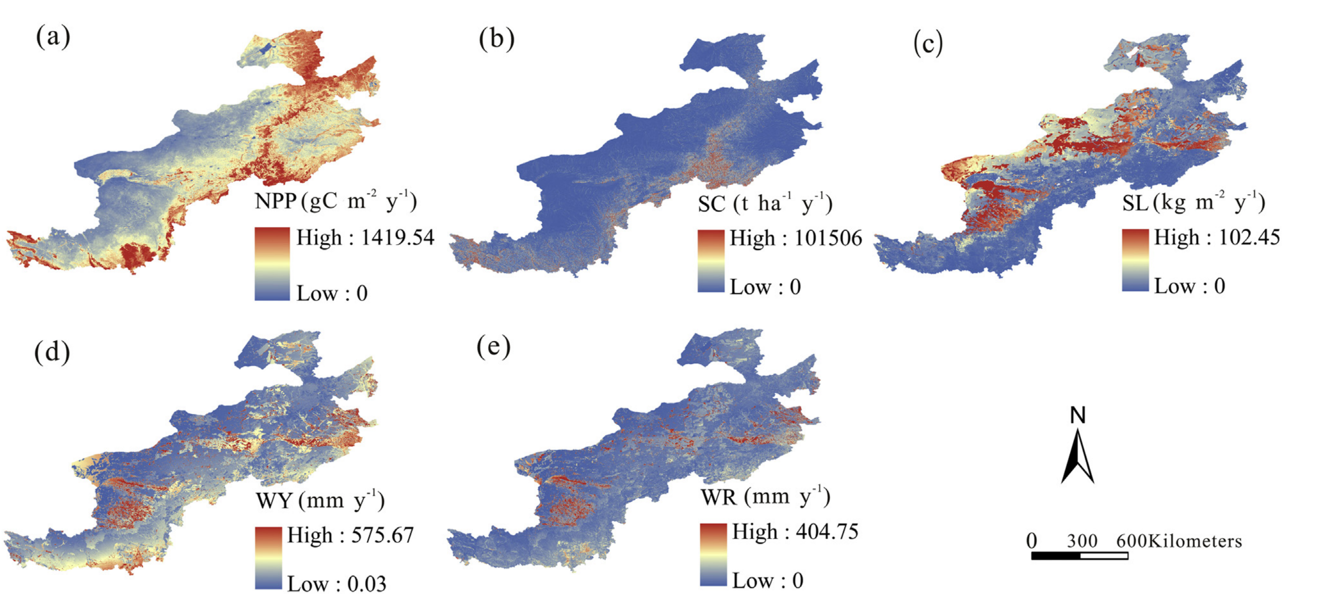

Fig. 5. The spatial pattern of five ecosystem services, including (a) net primary productivity, (b) soil conservation, (c) soil erosion by wind, (d) water yield, and (e) water retention in 2000.

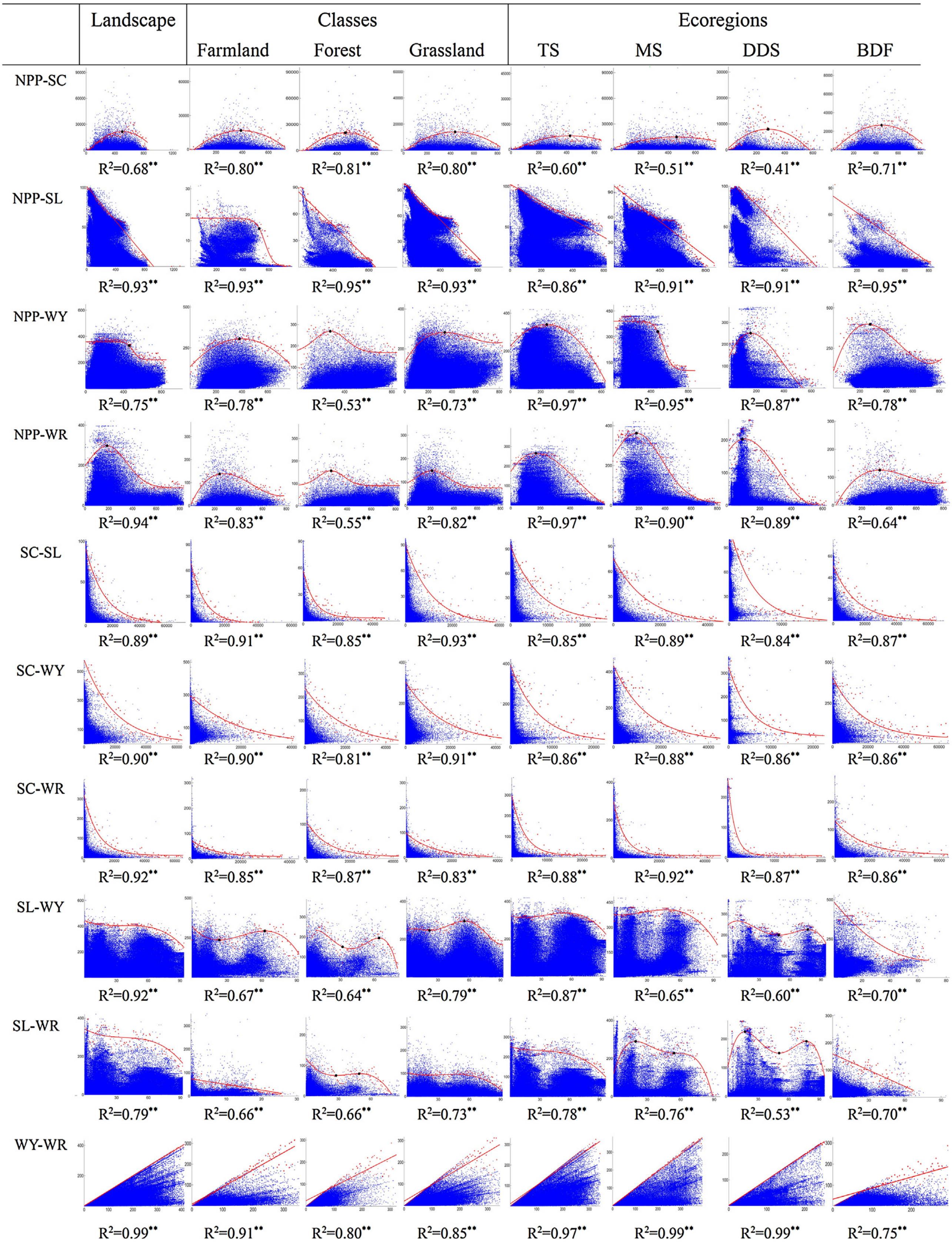

Fig. 6. Scatter plots (blue), boundary points (red), constraint lines (red), and thresholds (black points on constraint lines) of ten paired ecosystem services on the three levels of landscape, class, and ecoregion in 2000. Farmland, forest, and grassland are presented at the class level. We also show typical steppe (TS), meadow steppe (MS), desert and desert steppe (DDS), and broadleaf deciduous forest (BDF) at the ecoregion level. A-B are paired ecosystem services, in which A presents the service on the *x*-axis and B corresponds to the one on the *y*-axis of the scatter plots, R^2 is the goodness of fit, and ** indicates significance at the 0.01 level. (For interpretation of the references to colour in this figure legend, the reader is referred to the web version of this article.).

Table 2
Thresholds of the constraint lines for paired ecosystem services on the three levels of landscape, class, and ecoregion in 2000.

	Landscape	Class level			Ecoregion level			
		Farmland	Forest	Grassland	TS	MS	DDS	BDF
NPP-SC	(503,21497)	(390,16700)	(490,20411)	(439,14072)	(424,8112)	(461,14712)	(282,7946)	(451,26642)
NPP-SL		(525,15)						
NPP-WY	(460,329)	(394,305)	(279,268)	(339,283)	(239,340)	(474,326)	(158,251)	(278,398)
NPP-WR	(186,297)	(240,137)	(248,156)	(213,148)	(361,258)	(180,362)	(88,202)	(331,125)
SL-WY		(23,236) (62,292)	(31,150) (64,195)	(22,247) (55,295)			(49,199) (77,225)	
SL-WR			(28,67) (49,73)			(19,289) (54,227)	(17,225) (50,150) (77,191)	

*Farmland, forest, and grassland are presented at the class level. Typical steppe (TS), meadow steppe (MS), desert and desert steppe (DDS) and broadleaf deciduous forest (BDF) are included at the ecoregion level. A–B are paired ecosystem services, in which A presents the service on the *x*-axis and B corresponds to the one on the *y*-axis of the scatter plots. In (x,y), x is the A value at the threshold and y is B value at the threshold. The units of NPP, SC, SL, WY and WR are $g\,C\,m^{-2}$, $t\,ha^{-1}\,y^{-1}$, $kg\,m^{-2}\,y^{-1}$, $mm\,y^{-1}$ and $mm\,y^{-1}$, respectively.

synchronously with WY (Fig. 6). SL, WY, and WR decreased logarithmically when SC increased on all levels (Fig. 6). For the pairs of NPP-SC and NPP-WR, the constraint lines were all hump-shaped with obvious thresholds (Fig. 6 and Table 2).

The constraint effects of paired ecosystem services of NPP-SL, NPP-WY, SL-WY, and SL-WR varied with level (Fig. 6). Except in the farmland area, NPP negatively constrained SL on the other levels. There was no obvious constraint effect of NPP on SL when the NPP was lower than the threshold in farmland areas (Fig. 6). Except on the landscape level and in the MS ecoregion, where the constraint lines of NPP-WY were backward S-shaped, the constraint lines on the other levels were hump-shaped (Fig. 6). The constraint effects of SL on WY and WR were negative convex on the landscape level and convex-waved or concave-waved on the class and ecoregion levels (Fig. 6).

4. Discussion

On the constraint line, one ecological variable was constrained by the other, with minimal constraint by other factors (Evanylo and Sumner, 1987; Guo et al., 1998; Mills et al., 2009). Below the constraint line, the distribution of the scatter points was not determined by the constraint factors (Thomson et al., 1996). We found that there were constraint effects between paired ecosystem services of NPP, SC, SL, WY, and WR in the GAPTZ, which was different from the traditional tradeoff and synergy of ecosystem services in the current studies (Bennett et al., 2009; Jia et al., 2014; Zhang et al., 2015). We calculated Spearman correlation coefficients between paired ecosystem services (Table S.1). As Table S.1 indicated, apart from WY-WR and NPP-SL, the relationships of other paired ecosystem services vary with scale and the correlation is very weak. In addition, correlation analysis could not get the interaction thresholds between paired ecosystem services and the scatter clouds (Fig. 6) do not meet the assumption of variance homogeneity of correlation analysis. However, the constraint line approach can conquer these shortcomings and accurately describe the relationship between paired ecosystem services.

4.1. The mechanism of constraint effects between paired ecosystem services

4.1.1. The linear constraint types

The constraint effects of WY on WR were positively linear on all three levels. WR was one part of the retained WY (Sharp et al., 2015), such that WR synergistically changed with the trend of WY and would not be greater than WY. Zheng et al. (2014) found synergy between WY and WR in northern China. In general, a higher vegetation productivity meant a smaller amount of soil erosion by wind in the GAPTZ (Gong et al., 2014). Plants can reduce the wind speed, and the root systems of vegetation can enhance the ability of soil to resist erosion (Fryrear et al., 1998). Nevertheless, the constraint effect of NPP on SL varies with scale. On both landscape and ecoregion levels, there were negative linear constraint effects of NPP on SL, while in the farmland areas, there was almost no obvious constraint effect of NPP on SL. This may

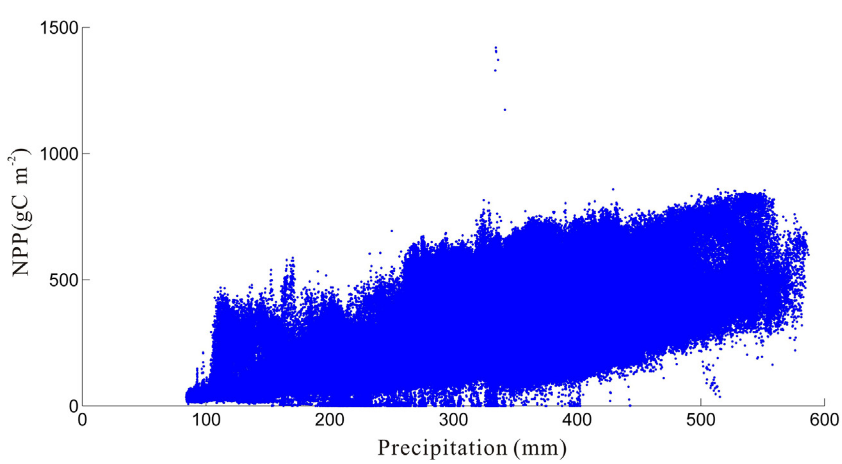

Fig. 7. The bivariate scatter plot of precipitation and net primary productivity (NPP) at landscape level in 2000.

occur because the protection from crop coverage and the damage from crop tillage offset one other. In the GAPTZ, current tillage practices for farmers to pursue high yield may result in greater damage on the soil's surface (Guo et al., 2013).

4.1.2. The logarithmic constraint type

SC has a logarithmic constraint effect on SL on all three levels, which indicated that soil erosion induced by water and wind were mutually exclusive in the study area. The sandy soil is easily eroded by both water and wind (Renard et al., 1991; Fryrear et al., 1998; Li, 1999). Runoff is the main driving force of SC (Wischmeier and Smith, 1965). When the precipitation was low, the land surface had less vegetation coverage (Fig. 7) and SC hardly occurred, but the opposite occurred for SL. Logarithmic constraint effects were also observed between SC and WY on all three levels. The water permeability of the sand was high, and only a small amount of precipitation could become runoff in the sand, while runoff easily occurs in clay (Zhou et al., 2005). Therefore, upon an increase in SC, WY decreases; Jia et al. (2014) and Zheng et al. (2014) found there is a tradeoff between SC and WY in arid and semi-arid areas of northern China. There were also logarithmic constraint effects of SC on WR on all three levels. The plant canopy and litter can intercept water and protect the soil from erosion.

4.1.3. The hump-shaped and the backward S-shaped constraint types

The constraint line is possibly shaped by an individual factor, but in most cases, it is shaped by multiple factors (Mills et al., 2009; Medinski et al., 2010). The relationship between NPP and SC may be impacted by multiple factors. On one hand, high NPP indicates good vegetation coverage, which can effectively protect the soil from erosion by water. On the other hand, over the NPP threshold (Fig. 7), a higher NPP also indicates a larger amount of precipitation, which increases the possibility of soil erosion by water. Jia et al. (2014) also showed the similar scatter plot pattern between NPP and SC in the arid areas of China. There were hump-shaped and backward S-shaped constraint effects of NPP on WY. WY is the portion of precipitation after subtracting evapotranspiration (Sharp et al., 2015). Evapotranspiration increases with plant growth (Jia et al., 2014; Cao et al., 2009; Cao et al., 2015). Below the NPP threshold, the precipitation was relatively low, and vegetation for all land uses did not grow well with low NPP (Fig. 7). In this case, WY and NPP synchronously increased with the increasing precipitation. However, in this arid and semiarid study area, evapotranspiration was very high, thus reducing water availability with vegetation growth and causing WY to decrease over the NPP threshold. Li et al. (2016) also found that evapotranspiration from restored vegetation led to the reduced runoff in the arid and semiarid areas in northern China. WR is the retained portion of WY, and the constraint effects of NPP on WY and WR were similar.

4.1.4. The convex-waved and concave-waved constraint types

The constraint effects of SL on WY and WR varied with scale (Fig. 6). In the sandy soil, the value of SL ranged from 0.004 $kg\,m^{-2}$ to 101 $kg\,m^{-2}$. The mean was 57 $kg\,m^{-2}$, which was much larger than the values found in other soil types. On the constraint lines, WY and WR slightly decreased with increases in SL. There are three potential reasons for this phenomenon. First, the main driving force of SL is the wind force. Wind can increase the evaporation, such that WY and WR decrease with an increase in SL. Second, precipitation is the main source of WY and WR in the study area and can prevent soil erosion by wind force, improving the vegetation quality and soil features. Finally, with stronger moisture permeability, the sandy soil in most of the study areas is easily blown away by the force of the wind. The convex-waved and concave-waved constraint lines indicated that the relationships between paired ecosystem services were relatively complex and may have been affected by many factors, such as soil type, precipitation, and wind force, among others.

The types of constraint lines in Fig. 3 (c, e, g, j) were not found in our case study, in which the relationships between paired ecosystem services were possibly dominated by individual or multiple factors.

4.2. Implications of the constraint line approach in managing ecosystem services

In the arid and semiarid areas, water availability is the most important constraint factor for maintaining NPP, SC, WY, and WR. As indicated in Fig. 6, WY and WR was able to achieve a win–win situation; the increases in WY, WR, and NPP were able to reduce SL, especially in a sand soil, such that the restoration of vegetation could conserve water and protect the surface soil from erosion. Farmland management measures, such as building wind barriers and no-tillage cultivation, are encouraged. However, species features and composition for the purpose of vegetation restoration should receive special care. The species with higher NPP is not the sole consideration when the locals try to optimize or maximize ecosystem services. When the NPP was over the thresholds, WY, WR, and SC decreased on all three levels (Fig. 6). In addition, soil features are important factors that may affect the constraint effects of SC on both WY and WR. Therefore, we should consider the NPP thresholds, soil features, water availability, and other socioeconomic and biophysical conditions in combination to balance the supply of NPP, WY, WR, and SC.

The constraint line approach has been a powerful tool in optimizing crop production (Webb, 1972; Evanylo and Sumner, 1987). According to our study, it has enormous potential to manage and optimize ecosystem services. A constraint line represents the efficiency frontier, similar to the meaning of Pareto Efficiency in economics (Thomson et al., 1996; Lester et al., 2013). The points on the constraint lines represent the best strategy that can maximize the supply of multiple ecosystem services.

Despite the advantages, the constraint line approach still has its limitations. The relationships between paired ecosystem services represented by the constraint lines may not indicate the response variable directly reacting to the constraint variable, and on the contrary, they may interact indirectly through biophysical processes, as indicated in this study. Only by integrating a constraint line approach with other analysis tools can we objectively understand the relationships between ecosystem services.

5. Conclusions

In this study, we predominantly found that the relationships between ecosystem services were not simple correlations that can be interpreted as tradeoffs or synergies, but rather, they were constraint effects, varying with spatial scales and landscape contexts. In reality, the relationships between ecosystem services may be affected by many socioeconomic and biophysical factors and are thus heterogeneous both in space and time. The constraint effects between the ten paired ecosystem services in our study can be classified as linear, logarithmic, negative convex, backward S-shaped, hump-shaped, convex-waved, and concave-waved. In our study area, water availability was the key constraint factor that affected the relationships between the ten paired ecosystem services on all three levels. Additionally, soil features, vegetation coverage, crop cultivation, and wind greatly contributed to the relationships between the ten paired ecosystem services. The constraint line approach can help policy makers pick out the dominant factors that affect the supply of multiple ecosystem services and provide an effective tool to optimize the regional land system.

Acknowledgments

This research was supported by the Program of National Natural Science Foundation of China (No.41571170), Fund for Creative Research Groups of National Natural Science Foundation of China (No. 41621061), the Program of Introducing Talents of Discipline to Universities (Grant No. B08008), and the Project of State Key Laboratory of Earth Surface Processes and Resources Ecology. Special thanks are given to the referees and the editors for their instructive comments, suggestions and editing for the manuscript.

Appendix A. Supplementary data

Supplementary data associated with this article can be found, in the online version, at http://dx.doi.org/10.1016/j.agee.2017.02.015.

References

Allen, R.G., Pereira, L.S., Raes, D., Smith, M., 1998. Crop evapotranspiration: guidelines for computing crop water requirements. FAO Irrig. Drain. Pap. 56.
Bai, Y., Zhuang, C., Ouyang, Z., Zheng, H., Jiang, B., 2011. Spatial characteristics between biodiversity and ecosystem services in a human-dominated watershed. Ecol. Complex. 8, 177–183.
Bennett, E.M., Peterson, G.D., Gordon, L.J., 2009. Understanding relationships among multiple ecosystem services. Ecol. Lett. 12, 1394–1404.
Blackburn, T.M., Lawton, J.H., Perry, J.N., 1992. A method of estimating the slope of upper bounds of plots of body size and abundance in natural animal assemblages. Oikos 65, 107–112.
Buergi, M., Silbernagel, J., Wu, J., Kienast, F., 2015. Linking ecosystem services with landscape history. Landsc. Ecol. 30, 11–20.
Butler, J.R.A., Wong, G.Y., Metcalfe, D.J., Honzak, M., Pert, P.L., Rao, N., van Grieken, M. E., Lawson, T., Bruce, C., Kroon, F.J., Brodie, J.E., 2013. An analysis of trade-offs between multiple ecosystem services and stakeholders linked to land use and water quality management in the Great Barrier Reef Agriculture Australia. Ecosyst. Environ. 180, 176–191.
Cade, B.S., Guo, Q.F., 2000. Estimating effects of constraints on plant performance with regression quantiles. Oikos 91, 245–254.
Cai, C., Ding, S., Shi, Z., Huang, L., Zhang, G., 2000. Study of applying USLE and geographical information system IDRISI to protect soil erosion in small watershed. J. Soil Water Conserv. 14, 19–24. doi:http://dx.doi.org/10.13870/j.cnki.stbcxb.2000.02.005.
Cao, S., Chen, L., Yu, X., 2009. Impact of China's grain for Grain Project on the landscape of vulnerable arid and semi-arid agricultural regions; a case study in northern Shaanxi province. J. Appl. Ecol. 46, 536–543. doi:http://dx.doi.org/10.1111/j.1365-2664.2008.01605.x.
Cao, Q., Yu, D., Georgescu, M., Han, Z., Wu, J., 2015. Impacts of land use and land cover change on regional climate: a case study in the argo-pastoral transitional zone of China. Environ. Res. Lett. 10 (12), 124025. doi:http://dx.doi.org/10.1088/1748-9326/10/12/124025.
Castro, A.J., Verburg, P.H., Martin-Lopez, B., Garcia-Llorente, M., Cabello, J., Vaughn, C.C., Lopez, E., 2014. Ecosystem service trade-offs from supply to social demand: a landscape-scale spatial analysis. Landsc. Urban Plann. 132, 102–110.
Costanza, R., d'Arge, R., De Groot, R., Farber, S., Grasso, M., Hannon, B., Limburg, K., Naeem, S., O'neill, R.V., Paruelo, J., 1998. The value of the world's ecosystem services and natural capital. Ecol. Econ. 1, 3–15.
Costanza, R., de Groot, R., Sutton, P., van der Ploeg, S., Anderson, S.J., Kubiszewski, I., Farber, S., Turner, R.K., 2014. Changes in the global value of ecosystem services. Global Environ. Change 26, 152–158.
Daily, G., 1997. Nature's Services: Societal Dependence on Natural Ecosystems. Island Press.
Evanylo, G., Sumner, M., 1987. Utilization of the boundary line approach in the development of soil nutrient norms for soybean production 1. Commun. Soil Sci. Plant Anal. 18, 1379–1401.
Favretto, N., Stringer, L.C., Dougill, A.J., Dallimer, M., Perkins, J.S., Reed, M.S., Atlhopheng, J.R., Mulale, K., 2016. Multi-criteria decision analysis to identify dryland ecosystem service trade-offs under different rangeland land uses. Ecosyst. Serv. 17, 142–151.
Fryrear, D., Saleh, A., Bilbro, J., Schomberg, H., Stout, J., Zobeck, T., 1998. Revised wind erosion equation (RWEQ): wind erosion and water conservation research unit. Tech. Bull. 1.
Fu, B.J., Zhao, W.W., Chen, L.D., Zhang, Q.J., LU, Y.H., Gulinck, H., Poesen, J., 2005. Assessment of soil erosion at large watershed scale using RUSLE and GIS: a case study in the Loess Plateau of China. Land Degrad. Dev. 16, 73–85.
Fu, B.J., Wang, S., Su, C., Forsius, M., 2013. Linking ecosystem processes and ecosystem services. Curr. Opin. Environ. Sustain. 5, 4–10.
Gao, S.Y., Ha, S., Pan, Y.Z., 2000. Causes of rapid expansion of blown-sand disaster and long-term trend of desertification in Northern China. J. Nat. Disasters 9, 31–37. doi:http://dx.doi.org/10.13577/j.jnd.2000.0305.
Goldstein, J.H., Caldarone, G., Duarte, T.K., Ennaanay, D., Hannahs, N., Mendoza, G., Polasky, S., Wolny, S., Daily, G.C., 2012. Integrating ecosystem-service tradeoffs into land-use decisions. Proc. Natl. Acad. Sci. U. S. A. 109, 7565–7570.
Gong, G., Liu, J., Shao, Q., Zhai, J., 2014. Sand-fixing function under the change of vegetation coverage in a wind erosion area in Northern China. J. Resour. Ecol. 5, 105–114. doi:http://dx.doi.org/10.5814/j.jssn.1674-764x.2014.02.002.
Guo, Q., Brown, J.H., Enquist, B.J., 1998. Using constraint lines to characterize plant performance. Oikos 83, 237–245.
Guo, Z., Zobeck, T.M., Zhang, K., Li, F., 2013. Estimating potential wind erosion of agricultural lands in northern China using the Revised Wind Erosion Equation and geographic information systems. J. Soil Water Conserv. 68, 13–21.
Horning, M., 2012. Constraint lines and performance envelopes in behavioral physiology: the case of the aerobic dive limit. Front. Physiol. 3.
Jansen, J.M., Pronker, A.E., Kube, S., Sokolowski, A., Sola, J.C., Marquiegui, M.A., Schiedek, D., Bonga, S.W., Wolowicz, M., Hummel, H., 2007. Geographic and seasonal patterns and limits on the adaptive response to temperature of European Mytilus spp. and Macoma balthica populations. Oecologia 154, 23–34.
Jia, X., Fu, B., Feng, X., Hou, G., Liu, Y., Wang, X., 2014. The tradeoff and synergy between ecosystem services in the grain-for-green areas in Northern Shaanxi, China. Ecol. Indic. 43, 103–113.
Jiang, L., Xiao, Y., Zheng, H., Ouyang, Z., 2016. Spatio-temporal variation of wind erosion in Inner Mongolia of China between 2001 and 2010. Chin. Geog. Sci. 26, 155–164. doi:http://dx.doi.org/10.1007/s11769-016-0797-y.
Jopke, C., Kreyling, J., Maes, J., Koellner, T., 2015. Interactions among ecosystem services across Europe: bagplots and cumulative correlation coefficients reveal synergies, trade-offs, and regional patterns. Ecol. Indic. 49, 46–52.
Lester, S.E., Costello, C., Halpern, B.S., Gaines, S.D., White, C., Barth, J.A., 2013. Evaluating tradeoffs among ecosystem services to inform marine spatial planning. Mar. Policy 38, 80–89.
Li, S., Liang, W., Fu, B., Lü, Y., Fu, S., Wang, S., Su, H., 2016. Vegetation changes in recent large-scale ecological restoration projects and subsequent impact on water resources in China's Loess Plateau. Sci. Total Environ. 569–570, 1031–1039. doi:http://dx.doi.org/10.1016/j.scitotenv.2016.06.141.
Li, Z., 1999. Wind tunnel simulation of flow velocity on the windward slope. Res. Soil Water Conserv. 6, 75–79.
Lu, N., Fu, B., Jin, T., Chang, R., 2014. Trade-off analyses of multiple ecosystem services by plantation along a precipitation gradient across Loess Plateau landscapes. Landsc. Ecol. 29, 1697–1708.
MA, 2005a. Ecosystems and Human Well-being. Island Press, Washington, DC.
MA, 2005b. Millennium Ecosystem, Assessment: Ecosystems and Human Well-being. Island Press, Washington, DC.
Medinski, T., Mills, A., Esler, K., Schmiedel, U., Jürgens, N., 2010. Do soil properties constrain species richness? Insights from boundary line analysis across several biomes in south western Africa. J. Arid Environ. 74, 1052–1060.
Mills, A., Fey, M., Gröngröft, A., Petersen, A., Medinski, T., 2006. Unravelling the effects of soil properties on water infiltration: segmented quantile regression on a large data set from arid south-west Africa. Soil Res. 44, 783–797.
Mills, A., Fey, M., Donaldson, J., Todd, S., Theron, L., 2009. Soil infiltrability as a driver of plant cover and species richness in the semi-arid Karoo, South Africa. Plant Soil 320, 321–332.
Potter, C.S., Randerson, J.T., Field, C.B., Matson, P.A., Vitousek, P.M., Mooney, H.A., Klooster, S.A., 1993. Terrestrial ecosystem production: a process model based on global satellite and surface data. Global Biogeochem. Cycles 7.
Qiu, J., Tang, H., 2003. Study on the situation of soil organic carbon storage in ecotone between agriculture and animal husbandry-a case study from Inner Mongolia. Chin. J. Eco-Agric. 11, 86–88.
Qiu, J., Turner, M.G., 2013. Spatial interactions among ecosystem services in an urbanizing agricultural watershed. Proc. Natl. Acad. Sci. 110, 12149–12154.
Raudsepp-Hearne, C., Peterson, G.D., Bennett, E.M., 2010. Ecosystem service bundles for analyzing tradeoffs in diverse landscapes. Proc. Natl. Acad. Sci. U. S. A. 107, 5242–5247.
Renard, K.G., Foster, G.R., Weesies, G.A., Porter, J.P., 1991. RUSLE: revised universal soil loss equation. J. Soil Water Conserv. 46, 30–33.
Roberts, J.H., Angermeier, P.L., 2007. Spatiotemporal variability of stream habitat and movement of three species of fish. Oecologia 151, 417–430.
Ruijs, A., Wossink, A., Kortelainen, M., Alkemade, R., Schulp, C.J.E., 2013. Trade-off analysis of ecosystem services in Eastern Europe. Ecosyst. Serv. 4, 82–94.
Sanon, S., Hein, T., Douven, W., Winkler, P., 2012. Quantifying ecosystem service trade-offs: the case of an urban floodplain in Vienna, Austria. J. Environ. Manage. 111, 159–172.
Sharp, R., Tallis, H.T., Ricketts, T., Guerry, A.D., Wood, S.A., Chaplin-Kramer, R., et al., 2015. InVEST + VERSION + User's Guide. The Natural Capital Project, Stanford University, University of Minnesota, The Nature Conservancy, and World Wildlife Fund.
Thomson, J.D., Weiblen, G., Thomson, B.A., Alfaro, S., Legendre, P., 1996. Untangling multiple factors in spatial distributions: lilies, gophers, and rocks. Ecology 77, 1698–1715.
Wang, J., Xu, X., Liu, P., 1999. Landuse and land carrying capacity in ecotone between agriculture and animal husbandry in northern China. Resour. Sci. 21, 19–24.
Webb, R., 1972. Use of the boundary line in the analysis of biological data. J. Hortic. Sci. 47, 309–319.

Wischmeier, W., Smith, D., 1965. Rainfall-erosion losses from cropland east of the rocky mountains, guide for selection of practices for soil and water conservation. Agric. Handb. 282.
Wong, C.P., Jiang, B., Kinzig, A.P., Lee, K.N., Ouyang, Z., 2015. Linking ecosystem characteristics to final ecosystem services for public policy. Ecol. Lett. 18, 108–118.
Wu, X., Akujärvi, A., Lu, N., Liski, J., Liu, G., Wang, Y., Holmberg, M., Li, F., Zeng, Y., Fu, B., 2015. Dynamics of soil organic carbon stock in a typical catchment of the Loess Plateau: comparison of model simulations with measurements. Landsc. Ecol. 30, 381–397.
Wu, J., 2004. Effects of changing scale on landscape pattern analysis: scaling relations. Landsc. Ecol. 19, 125–138.
Wu, J., 2013. Landscape sustainability science: ecosystem services and human well-being in changing landscapes. Landsc. Ecol. 28, 999–1023.
Zhang, X., Shi, P., 2003. Theory and practice of marginal ecosystem management-establishment of optimized eco-productive paradigm of grassland and farming-pastoral zone of north China. Acta Bot. Sin. 45, 1135–1138.
Zhang, L., Hickel, K., Dawes, W.R., Chiew, F.H., Western, A.W., Briggs, P.R., 2004. A rational function approach for estimating mean annual evapotranspiration. Water Resour. Res. 40, 89–97.
Zhang, L., Fu, B., Lü, Y., Zeng, Y., 2015. Balancing multiple ecosystem services in conservation. Landsc. Ecol. 30, 535–546.
Zheng, Z., Fu, B., Hu, H., Sun, G., 2014. A method to identify the variable ecosystem services relationship across time: a case study on Yanhe Basin, China. Landsc. Ecol. 29, 1689–1696.
Zhou, W., Liu, G., Pan, J., Feng, X., 2005. Distribution of available soil water capacity in China. J. Geog. Sci. 15, 3–12. doi:http://dx.doi.org/10.1007/BF02873101.
Zhu, W.Q., Pan, Y.Z., Zhang, J.S., 2007. Estimation of net primary productivity of Chinese terrestrial vegetation based on remote sensing. J. Plant Ecol. 31, 413–424.